Theor Chem Acc (2017) 136:113
DOI 10.1007/s00214-017-2149-0

REGULAR ARTICLE

Two-point weighted density approximations for the kinetic energy density functional

Debajit Chakraborty[1] · Rogelio Cuevas-Saavedra[1] · Paul W. Ayers[1]

Received: 27 July 2017 / Accepted: 17 September 2017 / Published online: 26 September 2017

Abstract We construct a model for the one-electron reduced density matrix that is symmetric and which satisfies the diagonal of the idempotency constraint and then use this model to evaluate the kinetic energy. This strategy for designing density functionals directly addresses the *N*-representability problem for kinetic energy density functionals. Results for atoms and molecules are encouraging, especially considering the simplicity of the model. However, like all of the other kinetic energy functionals in the literature, quantitative accuracy is not achieved.

Keywords Kinetic energy functional · Orbital-free density functional theory · Weighted density approximation · Model one-electron reduced density matrices

1 Motivation

Most modern density functional theory (DFT) calculations use the Kohn–Sham method, in which spin-orbitals are introduced as auxiliary functions for evaluating the kinetic energy [1]. Because the Kohn–Sham orbital occupation numbers are restricted to the interval [0,1], the Pauli principle is satisfied; this prevents the collapse of the system into an unphysical, nonfermionic, state [2–6]. However, computing the Kohn–Sham spin-orbitals requires solving a system of coupled, nonlinear, one-electron Schrödinger equations,

$$\left(-\tfrac{1}{2}\nabla^2 + v(\mathbf{r}) + v_J\left[\rho^\alpha, \rho^\beta;\mathbf{r}\right] + v_{xc}^\sigma\left[\rho^\alpha, \rho^\beta;\mathbf{r}\right]\right)\phi_i^\sigma(\mathbf{r}) = \varepsilon_i^\sigma \phi_i^\sigma(\mathbf{r}) \tag{1}$$

$$\rho^\sigma(\mathbf{r}) = \sum_i n_i^\sigma \left|\phi_i^\sigma(\mathbf{r})\right|^2 \qquad 0 \le n_i^\sigma \le 1 \tag{2}$$

The number of equations to be solved grows linearly with the number of electrons.

In principle, DFT calculations should only require determining one three-dimensional function (the electron density), not *N* three-dimensional functions (the Kohn–Sham spin-orbitals). This promise is realized in the orbital-free DFT approach [7–11]. The advantage of orbital-free DFT is especially clear when one writes the orbital-free equation for the square root of the electron (spin) density in the from proposed by Levy et al. [12],

$$\begin{aligned}&\left(-\tfrac{1}{2}\nabla^2 + v(\mathbf{r}) + v_J\left[\rho^\alpha, \rho^\beta;\mathbf{r}\right] + v_{xc}^\sigma\left[\rho^\alpha, \rho^\beta;\mathbf{r}\right]\right.\\ &\quad\left. + v_\theta^\sigma\left[\rho^\sigma;\mathbf{r}\right]\right)\varphi^\sigma(\mathbf{r}) = \varepsilon^\sigma\varphi^\sigma(\mathbf{r})\end{aligned} \tag{3}$$

$$\rho^\sigma(\mathbf{r}) = N^\sigma\left|\varphi^\sigma(\mathbf{r})\right|^2 \tag{4}$$

In orbital-free DFT, one needs to only solve one nonlinear Schrödinger equation [13–18]. (Or, in the spin-resolved DFT case, two coupled nonlinear Schrödinger equations). The number of equations to be solved is independent of the number of electrons.

The major problem in orbital-free DFT is the violation of the Pauli principle. This is clear from Eq. (3): if the Pauli potential, $v_\theta^\sigma(\mathbf{r})$, is omitted, the solution to Eq. (3) corresponds to a noninteracting system of bosons, where all the particles are in a single orbital. It is only the presence of the Pauli potential,

✉ Paul W. Ayers
ayers@chemistry.mcmaster.ca

[1] Department of Chemistry and Chemical Biology, McMaster University, Hamilton, ON, Canada

$$v_\theta^\sigma\left[\rho^\sigma;\mathbf{r}\right] = \frac{\delta T_\theta[\rho^\sigma]}{\delta\rho^\sigma(\mathbf{r})} = \frac{\delta T_s^\sigma[\rho^\sigma]}{\delta\rho^\sigma(\mathbf{r})} - \frac{\delta T_w^\sigma[\rho^\sigma]}{\delta\rho^\sigma(\mathbf{r})}, \tag{5}$$

that allows Eq. (3) to be consistent with Fermi statistics. In Eq. (5),

$$T_s^\sigma\left[\rho^\sigma\right] = \sum_i n_i^\sigma \left\langle \phi_i^\sigma \middle| -\tfrac{1}{2}\nabla^2 \middle| \phi_i^\sigma \right\rangle \tag{6}$$

and

$$T_w^\sigma[\rho^\sigma] = \left\langle \sqrt{\rho^\sigma(\mathbf{r})} \middle| -\tfrac{1}{2}\nabla^2 \middle| \sqrt{\rho^\sigma(\mathbf{r})} \right\rangle = N^\sigma \left\langle \varphi^\sigma(\mathbf{r}) \middle| -\tfrac{1}{2}\nabla^2 \middle| \varphi^\sigma(\mathbf{r}) \right\rangle \tag{7}$$

denote the Kohn–Sham and the Weizsäcker kinetic energies, respectively. The primary research topic in orbital-free DFT, then, is approximating the kinetic energy [7, 9, 10, 19–24] or, alternatively, the Pauli potential $v_\theta^\sigma(\mathbf{r})$ [25–32]. It is particularly important that the contribution of the Paul principle to the kinetic energy be captured precisely. The failure of orbital-free DFT functionals to respect the Pauli principle leads to qualitative problems. For example, many approximate orbital-free kinetic energy functionals give reasonable kinetic energies for the true Kohn–Sham density, but upon variational optimization of the energy, the shell structure of the electron density vanishes and the energy decreases. This decrease in energy indicates that there is some electron density, $\rho^\sigma(\mathbf{r}) \neq \rho^\sigma_{\text{exact}}(\mathbf{r})$, for which

$$\tilde{T}_s^\sigma\left[\rho^\sigma\right] < \sum_i n_i^\sigma \varepsilon_i^\sigma - \int \rho^\sigma(\mathbf{r}) v_s^\sigma(\mathbf{r}) d\mathbf{r} = T_s^\sigma\left[\rho^\sigma\right], \tag{8}$$

where $\tilde{T}_s^\sigma[\rho^\sigma]$ denotes the approximate kinetic energy functional and $v_s^\sigma(\mathbf{r})$ is the Kohn–Sham potential. Expression (8) indicates that the kinetic energy functional does not satisfy the Pauli principle [3]. That is, expression (8) indicates that $\tilde{T}_s^\sigma[\rho^\sigma]$ is not N-representable in the sense that there exists no fermion wavefunction or ensemble with the electron density $\rho^\sigma(\mathbf{r})$ and the kinetic energy $\tilde{T}_s^\sigma$.

It is essential that orbital-free kinetic energy functionals come very close to modeling the Pauli principle exactly. Even a tiny error in the occupation number of a core orbital or a high-lying virtual orbital will cause a massive error in Eq. (6) [2, 3].

The goal of this work is to explore a family of weighted density approximation functionals [33–35] that are designed to directly address the N-representability problem. The hope is that by imposing necessary conditions associated with the Pauli principle, we prevent the variational collapse of wavefunctions and reproduce the shell structure and other features in the electron density [25, 36–42,]. It is important to recognize that a functional can be N-representable but still be very inaccurate; in particular, it can give results for the kinetic energy that are far too high. Having a functional that is (approximately) N-representable is therefore necessary, but not sufficient, for the accuracy of the approximation.

In the next section, the weighted density approximations we will use are discussed. Numerical methods are revealed in Sect. 3, and results are presented in Sect. 4. Section 5 discusses our findings and concludes.

2 Weighted density approximation (WDA) for the 1-electron reduced density matrix (1-matrix)

2.1 The Kohn–Sham 1-matrix

In Kohn–Sham DFT, one explicitly constructs an N-representable 1-electron reduced density matrix (1-matrix) from the electron density. This can be achieved, for example, using the Levy constrained search [43–45],

$$T_s^\sigma[\rho] = \underbrace{\min}_{\left\{\gamma^\sigma \middle| \substack{\rho^\sigma(\mathbf{r})=\gamma^\sigma(\mathbf{r},\mathbf{r}) \\ \gamma^\sigma=(\gamma^\sigma)^2}\right\}} \iint \delta\left(\mathbf{r}-\mathbf{r}'\right)\left(-\tfrac{1}{2}\nabla_{\mathbf{r}}^2\gamma^\sigma\left(\mathbf{r},\mathbf{r}'\right)\right)d\mathbf{r}\,d\mathbf{r}' \tag{9}$$

$$\gamma_s^\sigma\left[\rho^\sigma;\mathbf{r},\mathbf{r}'\right] = \arg \underbrace{\min}_{\left\{\gamma^\sigma \middle| \substack{\rho^\sigma(\mathbf{r})=\gamma^\sigma(\mathbf{r},\mathbf{r}) \\ \gamma^\sigma=(\gamma^\sigma)^2}\right\}} \iint \delta\left(\mathbf{r}-\mathbf{r}'\right)\left(-\tfrac{1}{2}\nabla_{\mathbf{r}}^2\gamma^\sigma\left(\mathbf{r},\mathbf{r}'\right)\right)d\mathbf{r}\,d\mathbf{r}' \tag{10}$$

Among all idempotent 1-matrices with the correct electron density, Eq. (10) selects the one with the lowest kinetic energy. (There are alternative approaches; if one minimized the Hartree–Fock energy functional (instead of the kinetic energy), then one would obtain a different $\rho^\sigma(\mathbf{r}) \to \gamma^\sigma\left(\mathbf{r},\mathbf{r}'\right)$ mapping [46, 47]). As is clear from Eq. (10), the mapping between the electron density and the 1-matrix in Kohn–Sham DFT is implicit.

2.2 A general model for the 1-matrix

Every explicit, and therefore approximate, mapping between the electron density and the 1-matrix induces an orbital-free kinetic energy functional,

$$\tilde{T}_s^\sigma[\rho] = \iint \delta\left(\mathbf{r}-\mathbf{r}'\right)\left(-\tfrac{1}{2}\nabla_{\mathbf{r}}^2\tilde{\gamma}^\sigma\left[\rho^\sigma;\mathbf{r},\mathbf{r}'\right]\right)d\mathbf{r}\,d\mathbf{r}' \tag{11}$$

In this paper, we decorate the symbols for approximate functionals with ˜. This is the approach we pursue in this paper. We note, in passing, that any density-to-1-matrix mapping also implies an approximate exchange energy functional,

$$\tilde{E}_x^\sigma[\rho] = \frac{-1}{2} \iint \frac{\left|\tilde{\gamma}^\sigma\left[\rho^\sigma;\mathbf{r},\mathbf{r}'\right]\right|^2}{|\mathbf{r}-\mathbf{r}'|} d\mathbf{r}\, d\mathbf{r}'. \tag{12}$$

To use Eq. (11), one first needs to select a functional form for the 1-matrix. This 1-matrix needs to be easy to compute. Equation (11) has no utility unless it is much easier to determine the model 1-matrix than it is to solve for the exact Kohn–Sham 1-matrix using Eq. (10). The form we consider is

$$\tilde{\gamma}^\sigma\left[\rho^\sigma;\mathbf{r},\mathbf{r}'\right] = \sqrt{\rho^\sigma(\mathbf{r})\rho^\sigma(\mathbf{r}')}\tilde{g}\left(k_F^\sigma|\mathbf{r}-\mathbf{r}'|\right) \tag{13}$$

where the function $\tilde{g}(x)$ must satisfy

$$\begin{aligned} \tilde{g}(0) &= 1 \\ \tilde{g}'(0) &= 0 \\ \tilde{g}''(0) &< 0 \end{aligned} \tag{14}$$

In addition, for all physically achievable values of the argument, $x \geq 0$, we must have

$$-1 < \tilde{g}(x) \leq 1. \tag{15}$$

The 1-matrix form in Eq. (13) will not give idempotent density matrices for systems with more than two electrons unless $\tilde{g}(x) < 0$ for some values of x [48]. This 1-matrix form is potentially exact because one can choose the Fermi wave vector as the 6-dimensional function,

$$k_F^\sigma\left(\mathbf{r},\mathbf{r}'\right) \equiv \frac{\tilde{g}^{-1}\left(\frac{\gamma_s^\sigma\left[\rho^\sigma;\mathbf{r},\mathbf{r}'\right]}{\sqrt{\rho^\sigma(\mathbf{r})\rho^\sigma(\mathbf{r}')}}\right)}{|\mathbf{r}-\mathbf{r}'|}. \tag{16}$$

Equation (16) usually has many solutions because $\tilde{g}(x)$ is not invertible.

2.3 The 1-point model for the 1-matrix

In order for Eq. (13) to be useful as a density functional, one needs to write the Fermi wave vector, k_F^σ, as a functional of the electron density. In the local density approximation, one chooses the value of the Fermi wave vector in the uniform electron gas,

$$\tilde{k}_{\text{LDA}}^\sigma\left[\rho^\sigma;\mathbf{r}\right] = \left(6\pi^2\rho^\sigma(\mathbf{r})\right)^{1/3}. \tag{17}$$

Inserting Eq. (17) into Eq. (13) gives a model 1-matrix that depends on the value of the k_F at one point,

$$\tilde{\gamma}_{\text{1pt - LDA}}^\sigma\left(\mathbf{r},\mathbf{r}'\right) = \sqrt{\rho^\sigma(\mathbf{r})\rho^\sigma(\mathbf{r}')}\tilde{g}\left(\tilde{k}_{\text{LDA}}^\sigma(\mathbf{r})|\mathbf{r}-\mathbf{r}'|\right). \tag{18}$$

2.4 The 2-point model for the 1-matrix

This 1-point model gives a 1-matrix that is not Hermitian; $\tilde{\gamma}_{\text{1pt - LDA}}^\sigma\left(\mathbf{r},\mathbf{r}'\right) \neq \left(\tilde{\gamma}_{\text{1pt - LDA}}^\sigma\left(\mathbf{r}',\mathbf{r}\right)\right)^*$. We can symmetrize this expression using the p-mean [49, 50],

$$\tilde{\kappa}_F^\sigma\left(\mathbf{r},\mathbf{r}'\right) = \left(\frac{\left(k_F^\sigma(\mathbf{r})\right)^p + \left(k_F^\sigma\left(\mathbf{r}'\right)\right)^p}{2}\right)^{1/p} \tag{19}$$

This nonlocal symmetrized expression is effective [10, 49, 51–57] when one uses methods like the Chacon–Alvarellos–Tarazona [58] approach to construct models [11, 24, 49, 51–53, 55, 56, 58–66] for the kinetic energy consistent with the Lindhard response [67, 68]. Using Eq. (19) gives a symmetric model for the 1-matrix that depends on the value of k_F at two points,

$$\tilde{\gamma}_{\text{2pt - LDA}}^\sigma\left(\mathbf{r},\mathbf{r}'\right) = \sqrt{\rho^\sigma(\mathbf{r})\rho^\sigma(\mathbf{r}')}\tilde{g}\left(\tilde{\kappa}_{\text{LDA}}^\sigma\left(\mathbf{r},\mathbf{r}'\right)|\mathbf{r}-\mathbf{r}'|\right). \tag{20}$$

For $p > 0$, the value of the k_F is dominated by the larger of $k_F(\mathbf{r})$ and $k_F\left(\mathbf{r}'\right)$. For $p < 0$, the value of the k_F is dominated by the smaller of $k_F(\mathbf{r})$ and $k_F\left(\mathbf{r}'\right)$. Specific interesting cases are,

$$\begin{array}{lll} \max\left(k_F(\mathbf{r}), k_F\left(\mathbf{r}'\right)\right) & \ell_\infty\text{-mean} & p \to \infty \\ \sqrt{\frac{k_F^2(\mathbf{r})+k_F^2(\mathbf{r}')}{2}} & \text{root-mean-square} & p = 2 \\ \frac{k_F(\mathbf{r})+k_F(\mathbf{r}')}{2} & \text{arithmetic mean} & p = 1 \\ \sqrt{k_F(\mathbf{r})k_F(\mathbf{r}')} & \text{geometric mean} & p \to 0 \\ \frac{2k_F(\mathbf{r})k_F(\mathbf{r}')}{k_F(\mathbf{r})+k_F(\mathbf{r}')} & \text{harmonic mean} & p = -1 \\ \min\left(k_F(\mathbf{r}), k_F\left(\mathbf{r}'\right)\right) & \text{minimum} & p \to -\infty \end{array} \tag{21}$$

There are other ways to symmetrize the 1-matrix. (e.g., one can add the 1-matrix to its Hermitian transpose.) We chose Eq. (20) because the resulting form of the 1-matrix more nearly coincides with our intuition and because the other symmetrized forms that have been proposed do not seem to have ever been tested numerically [69, 70].

2.5 Kinetic energy from the 1-matrix models

If one substitutes

$$\tilde{\gamma}_{\text{1pt}}^\sigma\left(\mathbf{r},\mathbf{r}'\right) = \sqrt{\rho^\sigma(\mathbf{r})\rho^\sigma(\mathbf{r}')}\tilde{g}\left(k_F^\sigma(\mathbf{r})|\mathbf{r}-\mathbf{r}'|\right) \tag{22}$$

and

$$\tilde{\gamma}_{\text{2pt}}^\sigma\left(\mathbf{r},\mathbf{r}'\right) = \sqrt{\rho^\sigma(\mathbf{r})\rho^\sigma(\mathbf{r}')}\tilde{g}\left(\left[\frac{\left(k_F^\sigma(\mathbf{r})\right)^p + \left(k_F^\sigma\left(\mathbf{r}'\right)\right)^p}{2}\right]^{1/p}|\mathbf{r}-\mathbf{r}'|\right) \tag{23}$$

into Eq. (11) and evaluates the kinetic energy, one obtains

$$\tilde{T}_s^\sigma[\rho^\sigma] = \int \frac{\nabla\rho^\sigma(\mathbf{r})\cdot\nabla\rho^\sigma(\mathbf{r})}{8\rho^\sigma(\mathbf{r})}d\mathbf{r} - \frac{3\tilde{g}''(0)}{2}\int \rho^\sigma(\mathbf{r})\left(k_F^\sigma(\mathbf{r})\right)^2 d\mathbf{r}. \quad (24)$$

This expression does not depend on whether one uses the 1-point or the 2-point model. Equation (24) only depends on the model one chooses for $\tilde{g}(x)$ and the way one chooses a value for $k_F(\mathbf{r})$. It should be noted that this result is peculiar to the kinetic energy; the corresponding exchange energy functional gives different values depending on whether one uses $\tilde{\gamma}_{1\text{pt}}^\sigma(\mathbf{r},\mathbf{r}')$ or $\tilde{\gamma}_{2\text{pt}}^\sigma(\mathbf{r},\mathbf{r}')$.

2.6 Uniform electron gas model for $\tilde{g}\left(k_F|\mathbf{r}-\mathbf{r}'|\right)$

There are many possible choices for $\tilde{g}\left(k_F|\mathbf{r}-\mathbf{r}'|\right)$ that are consistent with the mild constraints mentioned in Sect. 2.2. The exact form of $\tilde{g}(x)$ is known for the uniform electron gas,

$$\tilde{g}_{\text{UEG}}(x) = 3\left(\frac{\sin(x) - x\cos(x)}{x^3}\right). \quad (25)$$

In this model,

$$\tilde{g}''_{\text{UEG}}(0) = -\frac{1}{5}. \quad (26)$$

By using this form, we ensure that all our kinetic energy functionals will be exact in the uniform electron gas limit.

2.7 Weighted density approximations for the Fermi wave vector, k_F

The simplest approximation for k_F is the aforementioned LDA, Eq. (17). If one substitutes $\tilde{k}_{\text{LDA}}^\sigma$ into Eq. (24), then one derives,

$$\tilde{T}_{\text{LDA}}^\sigma[\rho^\sigma] = \int \frac{\nabla\rho^\sigma(\mathbf{r})\cdot\nabla\rho^\sigma(\mathbf{r})}{8\rho^\sigma(\mathbf{r})}d\mathbf{r} + \int \frac{3\left(6\pi^2\right)^{2/3}}{10}\left(\rho^\sigma(\mathbf{r})\right)^{5/3}d\mathbf{r} \quad (27)$$

This gives the Thomas–Fermi plus *full* Weizsäcker functional [35, 71],

$$\tilde{T}_{\text{LDA}}[\rho^\alpha,\rho^\beta] = \tilde{T}_{\text{TF}+\text{W}}[\rho^\alpha,\rho^\beta] = \sum_{\sigma=\alpha,\beta} T_{\text{TF}}^\sigma[\rho^\sigma] + T_w^\sigma[\rho^\sigma]. \quad (28)$$

For atomic and molecular electron densities, this functional gives kinetic energies far above the true values [35, 65, 72].

The local density approximation for k_F should be reliable for nearly uniform electron densities, but atomic and molecular densities are far from uniform. It would be better to determine an "effective" value for k_F. Recall that the N-representability error in the kinetic energy functional is associated with the fact that the model 1-matrix is not idempotent. This suggests that we choose the "effective" value for k_F so that the model 1-matrix is idempotent. For example, the idempotency condition on the 1-point model is given as,

$$\int \tilde{\gamma}_{1\text{pt}}^\sigma(\mathbf{r},\mathbf{r}')\tilde{\gamma}_{1\text{pt}}^\sigma(\mathbf{r}',\mathbf{r}'')d\mathbf{r}' = \tilde{\gamma}_{1\text{pt}}^\sigma(\mathbf{r},\mathbf{r}'') \quad (29)$$

This is an underdetermined system of equations, with one equation for each pair of points, $(\mathbf{r},\mathbf{r}'')$, and one unknown for each point, $k_F^\sigma(\mathbf{r})$.[1] To avoid this difficulty, we consider only the diagonal part of the idempotency condition, $\mathbf{r}=\mathbf{r}''$. Then one has

$$\int \tilde{\gamma}_{1\text{pt}}^\sigma(\mathbf{r},\mathbf{r}')\tilde{\gamma}_{1\text{pt}}^\sigma(\mathbf{r}',\mathbf{r})d\mathbf{r}' = \rho^\sigma(\mathbf{r}). \quad (30)$$

This is equivalent to the requirement that the exchange hole,

$$h_x^{\sigma\sigma}(\mathbf{r},\mathbf{r}') = -\frac{\gamma^{\sigma\sigma}(\mathbf{r},\mathbf{r}')\gamma^{\sigma\sigma}(\mathbf{r}',\mathbf{r})}{\rho^\sigma(\mathbf{r})\rho^\sigma(\mathbf{r}')} \quad (31)$$

be properly normalized,

$$\int \rho^\sigma(\mathbf{r}')h_x^{\sigma\sigma}(\mathbf{r},\mathbf{r}')d\mathbf{r}' = -1 \quad (32)$$

By forcing Eq. (32), one ensures that the functional is self-interaction-free [73]. That is, each σ-spin electron hollows-out a 1-electron hole in its immediate vicinity, so that it interacts with only $N^\sigma - 1$ other σ-spin electrons. This requirement is in the spirit of the Pauli principle, though it is obviously weaker than the Pauli principle [since Eq. (30) does not imply Eq. (29)].

If one substitutes the form of the 1-point model 1-matrix into the diagonal idempotency condition, one obtains a set of uncoupled nonlinear equations for $k_F^\sigma(\mathbf{r})$, with one equation for each point,

$$\rho^\sigma(\mathbf{r})\int \rho^\sigma(\mathbf{r}')\left(\tilde{g}\left(\tilde{k}_{1\text{pt-WDA}}^\sigma(\mathbf{r})|\mathbf{r}-\mathbf{r}'|\right)\right)^2 d\mathbf{r}' = \rho^\sigma(\mathbf{r}) \quad (33)$$

Substituting $k_{1\text{pt-WDA}}^\sigma(\mathbf{r})$ into Eqs. (22) and (24) gives the 1-point weighted density approximation (1WDA) [33–35, 74, 75] to the 1-matrix and the kinetic energy,

$$\tilde{T}_{1\text{pt-WDA}}^\sigma[\rho^\sigma] = \int \frac{\nabla\rho^\sigma(\mathbf{r})\cdot\nabla\rho^\sigma(\mathbf{r})}{8\rho^\sigma(\mathbf{r})}d\mathbf{r} - \frac{3\tilde{g}''(0)}{2}\int \rho^\sigma(\mathbf{r})\left(\tilde{k}_{1\text{pt-WDA}}^\sigma(\mathbf{r})\right)^2 d\mathbf{r} \quad (34)$$

[1] Even if we had a more general, six-dimensional, model for the Fermi wave vector, forcing idempotency exactly would shift one back to Kohn–Sham-like computational cost and is therefore unacceptable in the context of orbital-free DFT.

If one substitutes the form of the 2-point model 1-matrix into the diagonal idempotency condition, one obtains a system of *coupled* nonlinear equations for $k_F^\sigma(\mathbf{r})$.

$$\rho^\sigma(\mathbf{r}) \int \rho^\sigma(\mathbf{r}') \left(\tilde{g}\left[\left(\frac{\left(\tilde{k}^\sigma_{\text{2pt-WDA}}(\mathbf{r})\right)^p + \left(\tilde{k}^\sigma_{\text{2pt-WDA}}(\mathbf{r}')\right)^p}{2} \right)^{1/p} |\mathbf{r}-\mathbf{r}'| \right] \right)^2 d\mathbf{r}' = \rho^\sigma(\mathbf{r}) \tag{35}$$

Substituting $\tilde{k}^\sigma_{\text{2pt-WDA}}(\mathbf{r})$ into Eq. (24) gives the 2-point weighted density approximation (2WDA) [74, 75]. The model exchange hole from the 2WDA is both self-interaction-free and symmetric; we might hope, then, that the resulting functionals are nearly N-representable. We note that using the same type of strategy to approximate the exchange and exchange-correlation energies gives good, if not breathtaking, results [48, 74–82].

3 Numerical methods

We computed the electron densities for small atoms (hydrogen through argon) and small molecules by performing all-electron calculations at the unrestricted Hartree–Fock level using the 6-311 ++G** basis set and the *Gaussian* program [83]. Then, using these densities, we computed the Thomas–Fermi kinetic energy functional [84, 85],

$$\tilde{T}_{\text{TF}}\left[\rho^\alpha, \rho^\beta\right] = \sum_{\sigma=\alpha,\beta} \int \frac{3\left(6\pi^2\right)^{2/3}}{10} \left(\rho^\sigma(\mathbf{r})\right)^{5/3} d\mathbf{r}, \tag{36}$$

the Weizsäcker kinetic energy functional [86],

$$\tilde{T}_w\left[\rho^\alpha, \rho^\beta\right] = \sum_{\sigma=\alpha,\beta} \int \frac{\nabla\rho^\sigma(\mathbf{r}) \cdot \nabla\rho^\sigma(\mathbf{r})}{8\rho^\sigma(\mathbf{r})} d\mathbf{r}, \tag{37}$$

the second-order gradient expansion approximation [87],

$$\tilde{T}_{\text{GEA2}}\left[\rho^\alpha, \rho^\beta\right] = \tilde{T}_{\text{TF}}\left[\rho^\alpha, \rho^\beta\right] + \frac{1}{9}\tilde{T}_w\left[\rho^\alpha, \rho^\beta\right] \tag{38}$$

and the TF + 1/5W approximation [88],

$$\tilde{T}_{\text{TF}+\frac{1}{5}\text{W}}\left[\rho^\alpha, \rho^\beta\right] = \tilde{T}_{\text{TF}}\left[\rho^\alpha, \rho^\beta\right] + \frac{1}{5}\tilde{T}_w\left[\rho^\alpha, \rho^\beta\right]. \tag{39}$$

In addition, we computed the three approximate functionals described in Sect. 2.6, each based on the model 1-matrix from the uniform electron gas, Eq. (25). These functionals are the local density approximation [equivalent to $\tilde{T}_{\text{TF}+\text{W}}\left[\rho^\alpha, \rho^\beta\right]$; cf. Eq. (28)], [35, 71], the 1WDA functional [cf. Eq. (34)] and the 2WDA functional.

All of the derivatives were performed analytically using the expression for the electron density in the Gaussian basis set. Numerical integrations were done using the Becke-Lebedev method; [89–93] we carefully adjusted the number of radial and angular grid points to ensure that the results we report are converged with respect to the integration grid.

In the conventional WDA (1WDA), the value of $\tilde{k}^\sigma_{\text{1pt-WDA}}(\mathbf{r})$ at each grid point was determined by solving the nonlinear equation associated with that grid point. To solve the nonlinear equation, we computed the Jacobian exactly and then used Newton's method, with a trust radius. In the 2-point WDA (2WDA), there is a system of nonlinear equations with the dimensionality of the integration grid. The Jacobian is extremely diagonally dominant, and the equations can be solved, for modest values of p in Eq. (19), but assuming the Jacobian is diagonal and then using Newton's method, again with a trust radius. Our best algorithm inverted the diagonal approximation to the Jacobian and then corrected this model for the inverse Jacobian using a limited-memory bad Broyden method. That approach converged rapidly, typically in ten to twenty iterations.

Using the solutions we obtained, we determined the value of p in the generalized p-mean for which the errors in the atomic kinetic energies were the smallest. The best results were obtained for $p = 5$. We used $p = 5$ for all subsequent calculations, even though we could have obtained better kinetic energies for the molecular systems had we used larger p values.

The equations for $\tilde{k}^\sigma_{\text{2pt-WDA}}(\mathbf{r})$ are very ill-conditioned when $p > 1$. Recalling Eq. (21), when $p > 1$,

$$\tilde{\kappa}^\sigma(\mathbf{r}, \mathbf{r}') = \left(\frac{\left(\tilde{k}^\sigma_{\text{2pt-WDA}}(\mathbf{r})\right)^p + \left(\tilde{k}^\sigma_{\text{2pt-WDA}}(\mathbf{r}')\right)^p}{2} \right)^{1/p} \tag{40}$$

will be very insensitive to the value of $\tilde{k}^\sigma_{\text{2pt-WDA}}(\mathbf{r}')$ when $\mathbf{r}'$ is far from the molecule. Since the values of $\tilde{k}^\sigma_{\text{2pt-WDA}}(\mathbf{r}')$ in the low-density regions of the molecule have very little effect on the value of the integral in Eq. (35), the 2WDA system of equations is effectively overdetermined; it is often

Table 1 Atomic kinetic energies obtained from Hartree–Fock functional (T_{HF}), Thomas–Fermi functional ($\tilde{T}_{\mathrm{TF}}$), Weizsäcker functional ($\tilde{T}_{w}$), second-order gradient expansion ($\tilde{T}_{\mathrm{GEA2}}$), TF + 1/5W ($\tilde{T}_{\mathrm{TF}+\frac{1}{5}\mathrm{W}}$), the local density approximation to the 1-matrix ($\tilde{T}_{\mathrm{LDA}}$), the one-point weighted density approximation ($\tilde{T}_{\mathrm{1pt\text{-}WDA}}$) and the two-point weighted density approximation ($\tilde{T}^{p=5}_{\mathrm{2pt\text{-}WDA}}$)

Atom	T_{HF}	$\tilde{T}_{\mathrm{TF}}$	$\tilde{T}_{w}$	$\tilde{T}_{\mathrm{GEA2}}$	$\tilde{T}_{\mathrm{TF}+\frac{1}{5}\mathrm{W}}$	$\tilde{T}_{\mathrm{LDA}}$	$\tilde{T}_{\mathrm{1pt\text{-}WDA}}$	$\tilde{T}^{p=5}_{\mathrm{2pt\text{-}WDA}}$	Error in $\tilde{T}^{p=5}_{\mathrm{2pt\text{-}WDA}}$
H	0.4598	0.2632	0.4599	0.3143	0.3552	0.7231	0.4599	0.4599	3.27E − 05
He	2.7339	2.4231	2.7339	2.7269	2.9699	5.1571	2.7340	2.7340	0.0002
Li	7.2010	6.4636	6.9612	7.2371	7.8559	13.4248	7.4108	7.4526	0.2516
Be	14.243	12.82	13.334	14.301	15.486	26.153	14.809	14.846	0.6031
B	24.122	21.61	21.547	24.003	25.919	43.156	25.002	24.98	0.8589
C	37.217	33.4	31.851	36.938	39.769	65.249	38.751	38.549	1.3325
N	53.863	48.095	43.154	52.889	56.725	91.249	55.24	54.7	0.8374
O	74.215	67.532	58.428	74.024	79.217	125.96	78.11	76.933	2.7173
F	98.751	89.456	72.445	97.506	103.95	161.90	102.01	99.981	1.2305
Ne	127.81	116.93	89.626	126.89	134.85	206.55	132.66	129.33	1.5199
Na	160.64	147.54	109.31	159.68	169.4	256.85	166.89	162.17	1.5369
Mg	198.19	182.55	131.24	197.13	208.79	313.79	206.06	199.64	1.4528
Al	240.4	221.89	155.32	239.15	252.96	377.22	249.92	241.5	1.0989
Si	287.24	265.58	181.48	285.75	301.88	447.06	298.50	287.77	0.5233
P	338.96	313.75	209.47	337.02	355.64	523.22	351.96	338.53	− 0.4282
S	395.62	367.01	240.10	393.68	415.03	607.11	411.14	394.65	− 0.9752
Cl	456.91	424.06	271.89	454.27	478.44	695.95	474.06	454.13	− 2.7723
Ar	523.71	486.82	306.28	520.85	548.07	793.1	543.42	519.59	− 4.1159
Average relative error (%)		− 10.7	− 23.9	− 2.3	4.5	65.4	3.4	1.3	
RMS relative error (%)		13.31	27.9	7.5	8.1	66.5	3.6	2.0	

All the energies are reported in atomic units (Hartree)

impossible to find values for $\tilde{k}^{\sigma}_{\mathrm{2pt\text{-}WDA}}(\mathbf{r}')$ that solve Eq. (41) exactly without violating the physical constraint that $\tilde{k}^{\sigma}_{\mathrm{2pt\text{-}WDA}}(\mathbf{r}') \geq 0$. To assess the accuracy of the numerical solution, we computed the normalization integral,

$$N = \iint \rho^{\sigma}(\mathbf{r})\rho^{\sigma}(\mathbf{r}')\left(\tilde{g}\left[\left(\frac{\left(\tilde{k}^{\sigma}_{F}(\mathbf{r})\right)^{p} + \left(\tilde{k}^{\sigma}_{F}(\mathbf{r}')\right)^{p}}{2}\right)^{1/p}|\mathbf{r}-\mathbf{r}'|\right]\right)^{2} \mathrm{d}\mathbf{r}\,\mathrm{d}\mathbf{r}' \tag{41}$$

for the various choices for the effective Fermi wave vector, $\tilde{k}^{\sigma}_{\mathrm{LDA}}$, $\tilde{k}^{\sigma}_{\mathrm{1pt\text{-}WDA}}$ and $\tilde{k}^{\sigma}_{\mathrm{2pt\text{-}WDA}}$. The first two choices will obviously give poor results but, in cases where the 2WDA equations, Eq. (35), can be very accurately solved, Eq. (41) should be exact. The goal of our method is to solve equations (35) as accurately as possible subject to the constraint that $\tilde{k}^{\sigma}_{\mathrm{2pt\text{-}WDA}}$ is nonnegative.

4 Results

The results for the kinetic energies of atoms and twelve small molecules are reported in Tables 1 and 2, respectively. The most remarkable feature of this data is the extreme inaccuracy of the results obtained when one makes the local density approximation to the 1-matrix, Eq. (27). The assumptions from which this functional is derived are the same as the assumptions on which the Thomas–Fermi functional is based, but it is an order of magnitude less accurate.

Approximating k_F using a weighted density approximation dramatically improves the results. Both the 1WDA and 2WDA functionals give results that are systematically too high; that is consistent with these functionals being almost N-representable. The 2WDA is significantly better than the 1WDA for atoms, but for molecules the two approaches are more comparable. The 2WDA is remarkably accurate for atoms; it is competitive with the best other functional we considered [the second-order gradient expansion approximation, Eq. (38)]. Neither WDA approach is competitive with

Table 2 Small-molecule kinetic energies obtained from Hartree–Fock functional (T_{exact}), Thomas–Fermi functional ($\tilde{T}_{\mathrm{TF}}$), Weizsäcker functional ($\tilde{T}_{w}$), second-order gradient expansion ($\tilde{T}_{\mathrm{GEA2}}$), TF + 1/5W ($\tilde{T}_{\mathrm{TF}+\frac{1}{5}\mathrm{W}}$), the local density approximation to the 1-matrix ($\tilde{T}_{\mathrm{LDA}}$), the one-point weighted density approximation ($\tilde{T}_{\mathrm{1pt\text{-}WDA}}$) and the two-point weighted density approximation ($\tilde{T}^{p=5}_{\mathrm{2pt\text{-}WDA}}$)

Molecule	T_{HF}	$\tilde{T}_{\mathrm{TF}}$	$\tilde{T}_{w}$	$\tilde{T}_{\mathrm{GEA2}}$	$\tilde{T}_{\mathrm{TF}+\frac{1}{5}\mathrm{W}}$	$\tilde{T}_{\mathrm{LDA}}$	$\tilde{T}_{\mathrm{1pt\text{-}WDA}}$	$\tilde{T}^{p=5}_{\mathrm{2pt\text{-}WDA}}$	Error in $\tilde{T}^{p=5}_{\mathrm{2pt\text{-}WDA}}$
BF_3	320.72	291.96	235.39	318.12	339.04	527.35	332.84	326.69	5.9659
CO	111.69	101.17	86.98	110.83	118.56	188.15	115.99	114.55	2.8553
CO_2	186.02	168.66	142.27	184.45	197.12	310.93	192.94	190.38	4.3529
H_2O	75.39	68.397	56.84	74.712	79.765	125.24	78.369	76.887	1.5003
H_2CO	112.75	102.16	87.349	111.86	119.63	189.51	117.3	115.67	2.9145
LiF	105.99	96.333	78.646	105.07	112.06	174.98	110.18	107.94	1.9508
LiH	7.7029	6.9194	7.4134	7.7431	8.4021	14.333	8.2243	8.1962	0.4932
NH_3	55.566	50.353	43.4116	55.176	59.035	93.764	58.093	57.12	1.5539
C_2H_6	78.044	70.75	63.043	77.755	83.358	133.79	82.201	81.121	3.0776
C_2H_4	76.941	69.687	62.404	76.621	82.168	132.09	80.758	79.828	2.8867
C_2H_2	75.971	68.762	61.649	75.612	81.092	130.41	79.496	78.672	2.7010
C_6H_6	227.74	206.43	183.61	226.83	243.15	390.04	238.27	236.31	8.5642
Average relative error (%)		− 9.4	− 22.7	0.8	6.5	65.7	2.6	3.0	
RMS relative error (%)		9.4	23.6	0.9	6.6	65.9	2.7	3.2	

All the energies are reported in atomic units (Hartree)

Table 3 Table comparing the kinetic energy contribution to the atomization energies for a set of 12 molecules, Eq. (42)

Molecule	$\Delta T^{\mathrm{atomization}}_{\mathrm{HF}}$	$\Delta\tilde{T}^{\mathrm{atomization}}_{\mathrm{TF}}$	$\Delta\tilde{T}^{\mathrm{atomization}}_{w}$	$\Delta\tilde{T}^{\mathrm{atomization}}_{\mathrm{GEA2}}$	$\Delta\tilde{T}^{\mathrm{atomization}}_{\mathrm{TF}+\frac{1}{5}\mathrm{W}}$	$\Delta\tilde{T}^{\mathrm{atomization}}_{\mathrm{LDA}}$	$\Delta\tilde{T}^{\mathrm{atomization}}_{\mathrm{1pt\text{-}WDA}}$	$\Delta\tilde{T}^{\mathrm{atomization}}_{\mathrm{2pt\text{-}WDA}}$
BF_3	− 2.8339	− 4.8969	0.4018	− 4.8523	− 4.8166	− 4.4952	− 5.7139	− 5.539
CO	− 1.3178	− 1.4329	1.9796	− 1.2129	− 1.037	0.5467	− 0.7375	− 0.6135
CO_2	− 2.0196	− 2.1498	4.3469	− 1.6668	− 1.2805	2.1971	− 0.5804	− 0.4781
H_2O	− 0.9162	− 1.1101	1.7236	− 0.9186	− 0.7654	0.6135	− 0.3617	− 0.0138
H_2CO	− 1.526	− 1.9787	2.4195	− 1.7098	− 1.4948	0.4408	− 1.2369	− 0.9225
LiF	− 0.9615	− 1.4748	− 0.3654	− 1.5154	− 1.5479	− 1.8402	− 2.152	− 1.8396
LiH	− 0.3174	− 0.4655	− 0.2707	− 0.4955	− 0.5196	− 0.7362	− 0.6817	− 0.6037
NH_3	− 0.9624	− 2.1782	0.3564	− 2.1386	− 2.1069	− 1.8218	− 2.4128	− 1.9451
C_2H_6	− 2.0184	− 3.613	1.9253	− 3.399	− 3.2279	− 1.6877	− 3.5948	− 2.8798
C_2H_4	− 1.7471	− 2.992	1.7776	− 2.7945	− 2.6365	− 1.2143	− 2.9405	− 1.8682
C_2H_2	− 1.4796	− 2.371	1.709	− 2.1811	− 2.0292	− 0.662	− 2.3046	− 2.8798
C_6H_6	− 4.6163	− 7.6011	6.4322	− 6.8864	− 6.3147	− 1.1689	− 7.1559	− 6.333
Average relative error		− 0.962	3.596	− 0.755	− 0.588	0.907	− 0.763	− 0.391
RMS relative error		1.294	4.534	1.104	0.988	1.933	1.466	1.205

The methods used are Hartree–Fock functional (T_{exact}), Thomas–Fermi functional ($\tilde{T}_{\mathrm{TF}}$), Weizsäcker functional ($\tilde{T}_{w}$), second-order gradient expansion ($\tilde{T}_{\mathrm{GEA2}}$), TF + 1/5W ($\tilde{T}_{\mathrm{TF}+\frac{1}{5}\mathrm{W}}$), the local density approximation to the 1-matrix ($\tilde{T}_{\mathrm{LDA}}$), the one-point weighted density approximation ($\tilde{T}_{\mathrm{1pt\text{-}WDA}}$) and the two-point weighted density approximation ($\tilde{T}^{p=5}_{\mathrm{2pt\text{-}WDA}}$). All the energies are reported in atomic units (Hartree)

the second-order gradient expansion for molecules, though WDA2 is still the second-best method we considered.

The 1-matrix is more localized and has a simpler form in atoms, so the simple uniform electron gas model for the 1-matrix might be much less accurate for molecules than it is for atoms. This would explain the disappointing results in Table 2; it also would explain the disappointing results for the errors in the kinetic energy contribution to the atomization energies,

$$\Delta\tilde{T}^{\mathrm{atomization}}_{s} = \sum_{\alpha\in\mathrm{atoms}} \tilde{T}_{s}\left[\rho_{\alpha}\right] - \tilde{T}_{s}\left[\rho_{\mathrm{molecule}}\right], \tag{42}$$

Table 4 For atoms, the normalization of different types of model density matrices, including the exact Hartree–Fock density matrix (HF), the local density approximation (LDA), the 1-point weighted density approximation (1WDA) and the 2-point weighted density approximation with $p = 5$ (2WDA)

Atoms	HF	LDA	1WDA	2WDA	Error (2WDA)	Max. abs. error in normalization
H	1.0000	0.2286	Exact	Exact	Exact	Exact
He	2.0001	0.6385	Exact	Exact	Exact	Exact
Li	3.0000	0.9479	2.5491	2.6790	− 0.3209	4.00856E − 04
Be	3.9999	1.4283	3.1188	3.8524	− 0.1476	2.28421E − 04
B	4.9999	1.9381	3.6848	4.9149	− 0.08507	2.55228E − 04
C	5.9999	8.502	8.0445	6.1180	0.1180	5.13794E − 05
N	6.9999	3.0743	4.8653	6.9032	− 0.0968	2.38088E − 04
O	7.9999	3.5729	5.5302	8.0218	0.0218	3.42978E − 04
F	8.9999	4.2362	6.0873	8.8816	− 0.1184	3.12419E − 04
Ne	10.0000	4.8459	6.7196	9.8865	− 0.1136	3.07957E − 04
Na	10.9999	5.2342	6.9347	10.7444	− 0.2556	2.64519E − 04
Mg	11.9999	5.7763	7.2295	11.8803	− 0.1197	1.69319E − 04
Al	13.0000	6.3144	7.5515	12.8991	− 0.1009	2.79699E − 04
Si	13.9999	6.8823	7.9746	13.9378	− 0.06215	3.49458E − 04
P	15.0000	7.5063	8.3491	14.8894	− 0.1106	2.02306E − 04
S	15.9999	8.0685	8.9528	16.0449	0.0449	2.49852E − 04
Cl	16.9999	8.7436	9.3449	16.8892	− 0.1108	2.62877E − 04
Ar	17.9999	9.3996	9.9114	17.9057	− 0.0943	2.41629E − 04

The last column states the maximum absolute error in normalization at any point during the last step of iteration. The Kohn–Sham results can be used to assess the accuracy of the six-dimensional integration grid. Results for atoms with no more than one electron of a given spin are essentially exact

Table 5 For molecules, the normalization of different types of model density matrices, including the exact Hartree–Fock density matrix (HF), the local density approximation (LDA), the 1-point weighted density approximation (1WDA) and the 2-point weighted density approximation with $p = 5$ (2WDA)

Molecule	HF	LDA	1WDA	2WDA	Error (2WDA)	Max. abs. error in normalization
BF_3	31.9959	16.1347	22.6334	31.9316	− 0.0643	2.36073E − 04
CO	13.9999	6.7593	10.0234	13.9129	− 0.0869	5.23547E − 04
CO_2	21.9994	11.0348	15.9207	21.932	− 0.0673	2.06136E − 04
H_2O	10.0001	4.7863	6.6806	9.9067	− 0.0934	3.78058E − 04
HCHO	15.99903	7.8303	11.33698	15.9275	− 0.0715	2.51132E − 04
LiF	11.9915	5.5715	8.4329	11.8833	− 0.1082	5.69642E − 04
LiH	3.9986	1.38595	3.49198	3.8717	− 0.1269	3.82933E − 04
NH_3	9.9986	4.7514	6.7718	9.9133	− 0.0852	5.38250E − 04
C_2H_6	18.0018	8.8715	12.8775	17.9334	− 0.0685	1.35380E − 04
C_2H_4	15.9974	7.7833	11.4812	15.9229	− 0.0745	2.87588E − 04
C_2H_2	13.9995	6.7069	10.1122	13.9265	− 0.07297	2.55714E − 04
C_6H_6	42.0013	21.9997	31.4696	41.9514	− 0.0499	1.21998E − 04

The last column states the maximum absolute error in normalization at any point during the last step of iteration. The Kohn–Sham results can be used to assess the accuracy of the six-dimensional integration grid

reported in Table 3. Except for the Weizsäcker functional, all the functionals we tested give similar results for the atomization energies. The errors, which are of the order of 1 Hartree (627 kcal/mol), are entirely inadequate for chemical problems.

Errors in the normalization integral, Eq. (41), are reported in Table 4 (atoms) and Table 5 (molecules). We looked to see whether the errors in the kinetic energy and/or the errors in the atomization kinetic energies could be correlated with the errors here. It is not true that larger errors for the kinetic energy correlate with larger errors in the normalization test. It does not seem that the failure to exactly solve the nonlinear equations for $\tilde{k}^{\sigma}_{2\text{pt-WDA}}$ can be invoked as an excuse for the imperfect results reported here. Note that, as expected, the normalization integrals for the LDA approximation to the

Table 6 Table reporting the maximum and minimum eigenvalues of the model 1-matrix for the argon atom

Maximum eigenvalue			Minimum eigenvalue		
LDA	1WDA	2WDA	LDA	1WDA	2WDA
1.2158	1.6413	1.7894	− 0.06926	− 0.05381	− 0.09812

1-matrix and the 1WDA are quite poor, though the 1WDA results are systematically better. The last column of Table 5 reports the maximum absolute error in Eq. (33).

These errors are quite small, but because of the large number of points in the numerical integration grids, the sum of the errors can be sizeable.

5 Discussion

In this work, we proposed a 2-point weighted density approximation (2WDA) and we tested the conventional weighted density approximation (1WDA) and the 2WDA for atoms and small molecules. The results are not remarkable, but the 2WDA is a major improvement over the 1WDA and the results are competitive with those from the (second-order) gradient expansion. We only tested the kinetic energy functionals for accurate electron densities and did not variationally optimize the energy with these functionals. This is suitable for a preliminary study, as it is necessary (but not sufficient) for accurate kinetic energy functionals. However, many functionals that perform well for accurate electron densities give poor results (e.g., densities which lack shell structure) when they are implemented variationally. We will need to test this in our future work.

The strength of the weighted density approximation approach is that one addresses the Pauli principle directly by (partially) imposing a subset of the idempotency conditions on a model 1-matrix. The resulting 1-matrix is self-interaction-free, but it is not idempotent. To test how far the matrix was from idempotent, we computed the natural orbital occupation numbers in the model 1-matrix. For the argon atom, the maximum and minimum occupations are presented in Table 6; Fig. 1 shows the spectrum of most highly occupied orbitals. Note that the 1-matrix we considered was resolved on the integration grid: the number of orbital occupation numbers is thus equal to the number of grid points. There are therefore thousands of occupation numbers, most of which are nearly zero.

None of the density matrices is close to idempotent. The primary violation of N-representability is associated with core orbitals that contain significantly more than one electron. Superficially, the violation of the Pauli principle is worse for the 2WDA 1-matrix than it is for the LDA or the 1WDA model 1-matrix. This may be related to the too-small normalization constants for the LDA and 1WDA 1-matrices in Table 4.

We consider these preliminary results. The WDA is a very flexible form, and certain approximations we made here are far from optimal. The most severe approximation we made was to choose the p value that defined the generalized mean to be a constant. By comparing optimal p values for different atoms, it is clear that it would be better to have a small p value in the tails of the electron density, but a larger

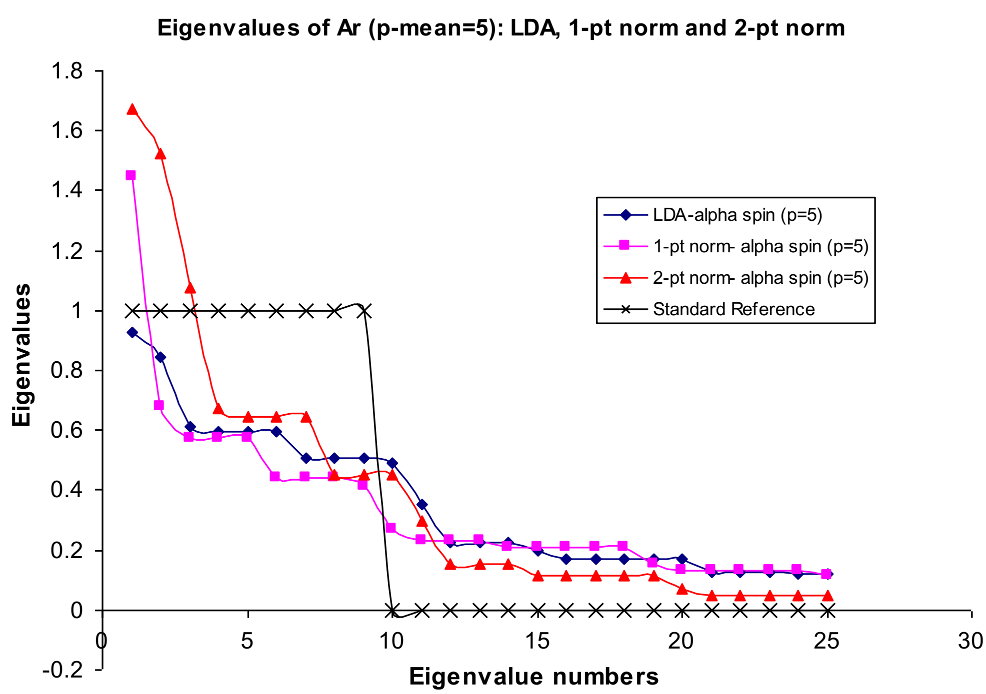

Fig. 1 Natural orbital occupation numbers for the model 1-matrix in the LDA, 1-point WDA and 2-point WDA approximations in the argon atom. In all cases, we symmetrized the 1-matrix [using Eq. (23)] before computing the eigenvalues

p value near the core. [This would also remedy the numerical difficulties in solving Eq. (35)]. Similarly, it is favorable to use a larger p value for molecules, where there is accumulation of density.

We would propose, then, to choose a hierarchy of models for p, in analogy to the "Jacob's ladder" of functionals in DFT [94–96]. By including information about the electron density (local density approximation for p) and its derivatives into p (generalized gradient approximations for p), we should be able to improve our model.

It will also be useful to consider more sophisticated forms for the model density matrix. The density matrix of atoms and molecules decays exponentially with increasing $|\mathbf{r}-\mathbf{r}'|$, [97, 98] so the uniform electron gas model we are using here decays far too slowly. By using a density matrix model that is more appropriate for atoms and molecules with a nonconstant value for p, it should be possible to improve the results obtained here significantly.

Acknowledgements Support from Sharcnet, NSERC, and the Canada Research Chairs is appreciated. RCS acknowledges financial support from CONACYT, ITESM and DGRI-SEP.

References

1. Kohn W, Sham LJ (1965) Self-consistent equations including exchange and correlation effects. Phys Rev 140:A1133–A1138
2. Manby FR, Knowles PJ, Lloyd AW (2001) Density matrix functional theory in average and relative coordinates. Chem Phys Lett 335:409–419
3. Ayers PW, Liu SB (2007) Necessary and sufficient conditions for the N-representability of density functionals. Phys Rev A 75:022514
4. Kryachko ES, Ludena EV (1991) Formulation of N-representable and upsilon-representable density-functional theory. 1. Groundstates. Phys Rev A 43:2179–2193
5. Ludena EV (2004) Is the Hohenberg–Kohn–Sham version of DFT a semi-empirical theory? J Mol Struct Theochem 709:25–29
6. Ludena EV, Illas F, Ramirez-Solis A (2008) On the N-representability and universality of F[ρ] in the Hohenberg–Kohn–Sham version of density functional theory. Int J Mod Phys B 22:4398
7. Karasiev VV, Jones RS, Trickey SB, Harris FE (2009) Recent advances in developing orbital-free kinetic energy functionals. In: Paz JL, Hernandez AJ (eds) New developments in quantum chemistry. Transworld Res Netw, Trivandrum
8. Chai JD, Weeks JD (2007) Orbital-free density functional theory: kinetic potentials and ab initio local pseudopotentials. Phys Rev B 75:205122. doi:10.1103/PhysRevB.75.205122
9. Wesolowski TA (2004) Quantum chemistry 'without orbitals'—an old idea and recent developments. Chimia 58(5):311–315
10. Wang YA, Carter EA, Schwartz SD (2000) Orbital-free kineticenergy density functional theory. In: Theoretical methods in condensed phase chemistry. Kluwer, Dordrecht, pp 117–184
11. GarciaGonzalez P, Alvarellos JE, Chacon E (1996) Nonlocal kinetic-energy-density functionals. Phys Rev B 53:9509–9512. doi:10.1103/PhysRevB.53.9509
12. Levy M, Perdew JP, Sahni V (1984) Exact differential-equation for the density and ionization-energy of a many-particle system. Phys Rev A 30:2745–2748
13. March NH (1985) Differential-equation for the ground-state density in finite and extended inhomogeneous electron gases. Phys Lett A 113(2):66–68
14. March NH (1986) The local potential determining the square root of the ground- state electron-density of atoms and molecules from the Schrodinger-equation. Phys Lett A 113(9):476–478
15. March NH (1986) Differential-equation for the electron-density in large molecules. Int J Quantum Chem 13:3–8
16. Kozlowski PM, March NH (1989) Approximate density external potential relation and the pauli potential for systems with coulombic interaction. Int J Quantum Chem 36(6):741–748
17. Levy M, Ouyang H (1988) Exact properties of the pauli potential for the square root of the electron-density and the kinetic-energy functional. Phys Rev A 38(2):625–629
18. Ayers PW, Parr RG (2003) Sufficient conditions for monotonic electron density decay in many-electron systems. Int J Quantum Chem 95:877–881
19. Chen HJ, Zhou AH (2008) Orbital-free density functional theory for molecular structure calculations. Numer Math Theory Methods Appl 1:1–28
20. Garcia-Aldea D, Alvarellos JE (2005) A study of kinetic energy density functionals: a new proposal. In: Simos T, Maroulis G (eds) Advances in computational methods in sciences and engineering 2005, vol 4A–4B. Lecture series on computer and computational sciences., pp 1462–1466
21. Iyengar SS, Ernzerhof M, Maximoff SN, Scuseria GE (2001) Challenge of creating accurate and effective kinetic-energy functionals. Phys Rev A 63(5):052508
22. Chan GKL, Handy NC (2000) An extensive study of gradient approximations to the exchange-correlation and kinetic energy functionals. J Chem Phys 112(13):5639–5653
23. Thakkar AJ (1992) Comparison of kinetic-energy density functionals. Phys Rev A 46:6920–6924. doi:10.1103/PhysRevA.46.6920
24. Garcia-Aldea D, Alvarellos JE (2007) Kinetic energy density study of some representative semilocal kinetic energy functionals. J Chem Phys 127:144109. doi:10.1063/1.2774974
25. Finzel K (2015) A simple approximation for the pauli potential yielding self-consistent electron densities exhibiting proper atomic shell structure. Int J Quantum Chem 115(23):1629–1634. doi:10.1002/qua.24986
26. Finzel K (2016) Local conditions for the Pauli potential in order to yield self-consistent electron densities exhibiting proper atomic shell structure. J Chem Phys 144(3):034108. doi:10.1063/1.4940035
27. Finzel K (2016) Reinvestigation of the ideal atomic shell structure and its application in orbital-free density functional theory. Theor Chem Acc 135(4):87. doi:10.1007/s00214-016-1850-8
28. Finzel K (2016) Approximating the Pauli potential in bound coulomb systems. Int J Quantum Chem 116(16):1261–1266. doi:10.1002/qua.25169
29. Finzel K, Davidsson J, Abrikosov IA (2016) Energy-surfaces from the upper bound of the pauli kinetic energy. Int J Quantum Chem 116(18):1337–1341. doi:10.1002/qua.25181
30. Finzel K, Ayers PW (2016) Functional constructions with specified functional derivatives. Theor Chem Acc 135(12):225. doi:10.1007/s00214-016-2013-7
31. Finzel K (2017) About the compatibility between ansatzes and constraints for a local formulation of orbital-free density functional theory. Int J Quantum Chem. doi:10.1002/qua.25329
32. Finzel K, Ayers PW (2017) The exact Fermi potential yielding the Hartree–Fock electron density from orbital-free density functional theory. Int J Quantum Chem. doi:10.1002/qua.25364
33. Gunnarsson O, Jonson M, Lundqvist BI (1977) Exchange and correlation in inhomogeneous electron-systems. Solid State Commun 24(11):765–768

34. Alonso JA, Girifalco LA (1977) Nonlocal approximation to exchange energy of non-homogenous electron-gas. Solid State Commun 24:135–138
35. Alonso JA, Girifalco LA (1978) Nonlocal approximation to exchange potential and kinetic-energy of an inhomogeneous electron-gas. Phys Rev B 17(10):3735–3743
36. Bader RFW, Gillespie RJ, Macdougall PJ (1988) A physical basis for the VSEPR model of molecular geometry. J Am Chem Soc 110:7329–7336
37. Wang W-P, Parr RG (1977) Statistical atomic models with piecewise exponentially decaying electron densities. Phys Rev A 16(3):891–902
38. de Silva P, Korchowiec J, Wesolowski TA (2014) Atomic shell structure from the single-exponential decay detector. J Chem Phys 140:164301
39. de Silva P, Korchowiec J, Ram JSN, Wesolowski TA (2013) Extracting information about chemical bonding from molecular electron densities via single exponential decay detector (SEDD). Chimia 67:253–256
40. de Silva P, Korchowiec J, Wesolowski TA (2012) Revealing the bonding pattern from the molecular electron density using single exponential decay detector: an orbital-free alternative to the electron localization function. Chem Phys Chem 13:3462–3465
41. Ayers PW (2005) Electron localization functions and local measures of the covariance. J Chem Sci 117:441–454
42. Tsirelson V, Stash A (2002) Determination of the electron localization function from electron density. Chem Phys Lett 351:142–148
43. Levy M (1979) Universal variational functionals of electron-densities, 1st-order density-matrices, and natural spin-orbitals and solution of the v-representability problem. Proc Natl Acad Sci 76:6062–6065
44. Levy M, Perdew JP (1985) The constrained search formulation of density functional theory. NATO ASI Series, Series B 123. Density Funct Methods Phys 11–30
45. Levy M (1996) Elementary concepts in density functional theory. Theor Comput Chem 4. Recent Developments and Applications of Modern Density Functional Theory 3–24
46. Gorling A, Levy M (1992) Requirements for correlation-energy density functionals from coordinate transformations. Phys Rev A 45:1509–1517
47. Gorling A, Levy M (1997) Hybrid schemes combining the Hartree–Fock method and density-functional theory: underlying formalism and properties of correlation functionals. J Chem Phys 106:2675–2680
48. Ayers PW, Cuevas-Saavedra R, Chakraborty D (2012) Phys Lett A 376:839–844. doi:10.1016/j.physleta.2012.01.028
49. GarciaGonzalez P, Alvarellos JE, Chacon E (1996) Kinetic-energy density functional: atoms and shell structure. Phys Rev A 54:1897–1905
50. Garcia-Gonzalez P, Alvarellos JE, Chacon E, Tarazona P (2000) Image potential and the exchange-correlation weighted density approximation functional. Phys Rev B 62:16063–16068. doi:10.1103/PhysRevB.62.16063
51. Garcia-Aldea D, Alvarellos JE (2007) Kinetic-energy density functionals with nonlocal terms with the structure of the Thomas–Fermi functional. Phys Rev A 76:052504. doi:10.1103/PhysRevA.76.052504
52. Garcia-Aldea D, Alvarellos JE (2008) Approach to kinetic energy density functionals: nonlocal terms with the structure of the von Weizsacker functional. Phys Rev A 77:022502. doi:10.1103/PhysRevA.77.022502
53. Garcia-Aldea D, Alvarellos JE (2008) Fully nonlocal kinetic energy density functionals: a proposal and general assessment for atomic systems. J Chem Phys 129:074103
54. Garcia-Gonzalez P, Alvarellos JE, Chacon E (1998) Kinetic-energy density functionals based on the homogeneous response function applied to one-dimensional fermion systems. Phys Rev A 57(6):4192–4200
55. Wang YA, Govind N, Carter EA (1999) Orbital-free kinetic-energy density functionals with a density-dependent kernel. Phys Rev B 60:16350–16358
56. Zhou BJ, Ligneres VL, Carter EA (2005) Improving the orbital-free density functional theory description of covalent materials. J Chem Phys 122:044103. doi:10.1063/1.1834563
57. Garcia-Gonzalez P, Alvarellos JE, Chacon E (1998) Nonlocal symmetrized kinetic-energy density functional: application to simple surfaces. Phys Rev B 57:4857–4862. doi:10.1103/PhysRevB.57.4857
58. Chacon E, Alvarellos JE, Tarazona P (1985) Nonlocal kinetic-energy functional for nonhomogeneous electron-systems. Phys Rev B 32:7868–7877
59. Wang LW, Teter MP (1992) Kinetic-energy functional of the electron-density. Phys Rev B 45:13196–13220. doi:10.1103/PhysRevB.45.13196
60. Smargiassi E, Madden PA (1994) Orbital-free kinetic-energy functionals for 1st-principles molecular-dynamics. Phys Rev B 49:5220–5226. doi:10.1103/PhysRevB.49.5220
61. Perrot F (1994) Hydrogen–hydrogen interaction in an electron-gas. J Phys: Condens Matter 6:431–446. doi:10.1088/0953-8984/6/2/014
62. Wang YA, Govind N, Carter EA (1998) Orbital-free kinetic-energy functionals for the nearly free electron gas. Phys Rev B 58:13465–13471
63. Huang C, Carter EA (2010) Nonlocal orbital-free kinetic energy density functional for semiconductors. Phys Rev B 81:045206. doi:10.1103/PhysRevB.81.045206
64. Ovchinnikov IV, Bartell LA, Neuhauser D (2007) Hydrodynamic tensor density functional theory with correct susceptibility. J Chem Phys 126(13):134101
65. Herring C (1986) Explicit estimation of ground-state kinetic energies from electron-densities. Phys Rev A 34:2614–2631. doi:10.1103/PhysRevA.34.2614
66. Genova A, Pavanello M (2017) Nonlocal kinetic energy functionals by functional integration. arxiv: 1704.08943
67. Lindhard J (1954) K Dan Vidensk Selsk Mat-Fys Medd 28:8
68. Pick RM, Cohen MH, Martin RM (1970) Microscopic theory of force constants in the adiabatic approximation. Phys Rev B 1:910
69. Wang YA (1997) Natural variables for density functionals. Phys Rev A 55(6):4589–4592
70. Wu ZG, Cohen RE, Singh DJ (2004) Comparing the weighted density approximation with the LDA and GGA for ground-state properties of ferroelectric perovskites. Phys Rev B 70:104112. doi:10.1103/PhysRevB.70.104112
71. Katsumi Y (1967) Energy levels for an extended Thomas–Fermi–Dirac potential. J Phys Soc Jpn 22:1127–1132
72. Murphy DR, Wang WP (1980) Comparative-study of the gradient expansion of the atomic kinetic-energy functional-neutral atoms. J Chem Phys 72(1):429–433
73. Perdew JP, Zunger A (1981) Self-interaction correction to density-functional approximations for many-electron systems. Phys Rev B 23:5048–5079
74. Cuevas-Saavedra R, Chakraborty D, Rabi S, Cardenas C, Ayers PW (2012) Symmetric non local weighted density approximations from the exchange-correlation hole of the uniform electron gas. J Chem Theory Comput 8(11):4081–4093. doi:10.1021/ct300325t
75. Cuevas-Saavedra R, Chakraborty D, Ayers PW (2012) Symmetric two-point weighted density approximation for exchange energies. Phys Rev A 85(4):042519. doi:10.1103/PhysRevA.85.042519

76. Cuevas-Saavedra R, Thompson DC, Ayers PW (2016) Alternative Ornstein–Zernike models from the homogeneous electron liquid for density functional theory calculations. Int J Quantum Chem 116(11):852–861. doi:10.1002/qua.25081
77. Cuevas-Saavedra R, Ayers PW (2012) Using the spin-resolved electronic direct correlation function to estimate the correlation energy of the spin-polarized uniform electron gas. J Phys Chem Solids 73:670–673. doi:10.1016/j.jpcs.2012.01.004
78. Cuevas-Saavedra R, Ayers PW (2012) Addressing the Coulomb potential singularity in exchange-correlation energy integrals with one-electron and two-electron basis sets. Chem Phys Lett 539:163–167. doi:10.1016/j.cplett.2012.04.037
79. Antaya H, Zhou YX, Ernzerhof M (2014) Approximating the exchange energy through the nonempirical exchange-factor approach. Phys Rev A 90(3):032513. doi:10.1103/PhysRevA.90.032513
80. Patrick CE, Thygesen KS (2015) Adiabatic-connection fluctuation-dissipation DFT for the structural properties of solids-the renormalized ALDA and electron gas kernels. J Chem Phys 143(10):102802. doi:10.1063/1.4919236
81. Zhou YX, Bahmann H, Ernzerhof M (2015) Construction of exchange-correlation functionals through interpolation between the non-interacting and the strong-correlation limit. J Chem Phys 143(12):124103. doi:10.1063/1.4931160
82. Precechtelova JP, Bahmann H, Kaupp M, Ernzerhof M (2015) Design of exchange-correlation functionals through the correlation factor approach. J Chem Phys 143(14):144102. doi:10.1063/1.4932074
83. Frisch MJ, Trucks GW, Schlegel HB, Scuseria GE, Robb MA, Cheeseman JR, Scalmani G, Barone V, Mennucci B, Petersson GA, Nakatsuji H, Caricato M, Li X, Hratchian HP, Izmaylov AF, Bloino J, Zheng G, Sonnenberg JL, Hada M, Ehara M, Toyota K, Fukuda R, Hasegawa J, Ishida M, Nakajima T, Honda Y, Kitao O, Nakai H, Vreven T, Montgomery JA Jr, Peralta JE, Ogliaro F, Bearpark M, Heyd JJ, Brothers E, Kudin KN, Staroverov VN, Kobayashi R, Normand J, Raghavachari K, Rendell A, Burant JC, Iyengar SS, Tomasi J, Cossi M, Rega N, Millam JM, Klene M, Knox JE, Cross JB, Bakken V, Adamo C, Jaramillo J, Gomperts R, Stratmann RE, Yazyev O, Austin AJ, Cammi R, Pomelli C, Ochterski JW, Martin RL, Morokuma K, Zakrzewski VG, Voth GA, Salvador P, Dannenberg JJ, Dapprich S, Daniels AD, Farkas O, Foresman JB, Ortiz JV, Cioslowski J, Fox DJ (2009) Gaussian 09, Revision A.1. Gaussian Inc., Wallingford
84. Thomas LH (1927) The calculation of atomic fields. Proc Camb Philos Soc 23:542–548
85. Fermi E (1928) A statistical method for the determination of some atomic properties and the application of this method to the theory of the periodic system of elements. Z Phys 48:73–79
86. Von Weizsacker CF (1935) Zur theorie dier kernmassen. ZPhysik 96:431–458
87. Kirzhnits DA (1957) Quantum corrections to the Thomas–Fermi equation. Sov Phys JETP 5:64–71
88. Berk A (1983) Lower-bound energy functionals and their application to diatomic systems. Phys Rev A 28:1908–1923. doi:10.1103/PhysRevA.28.1908
89. Becke AD (1988) A multicenter numerical-integration scheme for polyatomic molecules. J Chem Phys 88:2547–2553
90. Lebedev VI (1975) Spherical quadrature formulas exact to orders 25–29. Sibirskii Matematicheskii Zhurnal 18:99–107
91. Lebedev VI (1992) Quadrature formulas of orders 41, 47, and 53 for the sphere. Russ Acad Sci Dokl Math 45:587–592
92. Lebedev VI (1992) A quadrature formula for the sphere of 59th algebraic order of accuracy. Russ Acad Sci Dokl Math 50:283–286
93. Lebedev VI, Laikov DN (1999) Quadrature formula for the sphere of 131-th algebraic order of accuracy. Dokl Akad Nauk 366:741–745
94. Tao JM, Perdew JP, Staroverov VN, Scuseria GE (2003) Climbing the density functional ladder: nonempirical meta-generalized gradient approximation designed for molecules and solids. Phys Rev Lett 91:146401
95. Perdew JP, Ruzsinszky A, Tao JM, Staroverov VN, Scuseria GE, Csonka GI (2005) Prescription for the design and selection of density functional approximations: more constraint satisfaction with fewer fits. J Chem Phys 123:062201
96. Goerigk L, Grimme S (2011) A thorough benchmark of density functional methods for general main group thermochemistry, kinetics, and noncovalent interactions. PCCP 13:6670–6688. doi:10.1039/c0cp02984j
97. Kohn W (1996) Density functional and density matrix method scaling linearly with the number of atoms. Phys Rev Lett 76:3168–3171
98. He LX, Vanderbilt D (2001) Exponential decay properties of Wannier functions and related quantities. Phys Rev Lett 86:5341–5344